Dealing with actuator rate limits. Towards IQC-based analysis of aircraft-pilot system stability

Ioan URSU*,[1], Adrian TOADER[1]

*Corresponding author
[1]INCAS − National Institute for Aerospace Research "Elie Carafoli"
B-dul Iuliu Maniu 220, Bucharest 061126, Romania
iursu@incas.ro*, atoader@incas.ro

DOI: 10.13111/2066-8201.2013.5.2.7

Abstract: *The study continues the recent work of the authors, by sketching an approach of the aircraft-pilot system stability analysis, considering both the rate saturation of the actuator and the time delay in control input. A stable behavior of the closed loop pilot-aircraft system with input delay was previously obtained. The problem is now if this stability survives in the presence of the actuator rate saturation. The mathematical tools of stability analysis are those of the Integral Quadratic Constraints (IQC) methodology.*

Key Words: *LQG control, optimal model of human pilot, PIO, input delay, actuator rate limit, Kalman-Yakubovich-Popov Lemma*

1. INTRODUCTION

Absolute stability, as was introduced and defined in [1], is in fact a global asymptotic stability of the equilibrium of a feedback system with a special structure, consisting of a loop of some linear (L) and nonlinear (N) components (Fig. 1a). Asymptotic stability is global in the sense that it refers to a whole class of functions that define the nonlinear component (N). We mention in passing that absolute stability theory was developed around Aizerman [2] and Kalman's [3] conjectures which, although disproved, were fruitful for the applications of the problem they have generated.

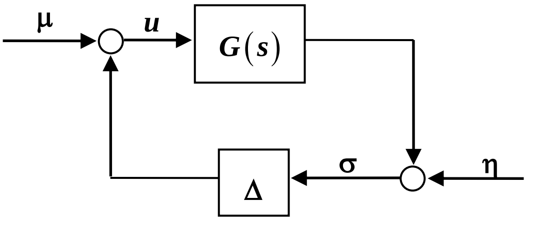

Fig. 1 – Basic feedback configuration of IQC paradigm

One of the most consistent achievements of the absolute stability theory continues to be over 50 years the frequency stability criterion of Popov [4]. Certainly, it was expressed only as a sufficient condition, as the other contributions that have followed (for example, the circle criterion, see, e.g., [5]). Therefore, a challenge faced by researchers over time was to reduce the conservatism inherent to any theorem expressed as a sufficient condition, in other words, to reduce the "distance" between a sufficient condition and a sufficient and necessary condition. A common idea was this: more restrictions will be imposed on the nonlinear part N of the system, less restrictive (therefore, less conservative) will be the conditions on the linear part L defined by the frequency domain inequality or by the equivalent to it Liapunov function [6] (see also [7]). This research direction has resulted in so-called Integral Quadratic Constraints (IQC) method, as it is known today through the work of Megretski and Rantzer [8]. As shown in [9], the IQC theory has its roots in at least three fruitful research fields: the *input-output theory* (Zames and Falb [10], Willems [11]); the *absolute stability theory* with special contributions from Popov [4] and Yakubovich [12]; the *robust control* ([13], [14], etc.). Here is added a less known book of Rasvan [15], with real contributions at the time.

The stability of the closed loop pilot-aircraft system is important from both theoretical and practical viewpoint, and it is herein put in touch with a timeliness problem, that of prediction and prevention of the Pilot Induce Oscillations (PIO) phenomenon. PIO is usually due to adverse aircraft-pilot coupling during some tasks in which "tight closed loop control of the aircraft is required from the pilot, with the aircraft not responding to pilot commands as expected by the pilot himself" [16]. Predicting PIO is, of course, difficult and becomes even more difficult with the advent of new technologies such as active control and fly-by-wire flight control systems. According to common references (e.g., [17]), PIO phenomenon is categorized depending essentially on the degree of nonlinearity of the different circumstances. In the category PIO II, quasi-linear oscillations result mainly from rate and/or position saturation of the actuator.

In terms of input-state-output space representation, when modelling PIO, a state model of human pilot must be introduced in conjunction with the aircraft model. Clearly, the output of the pilot is the input to the aircraft model, but this junction follows to be fatalistically corrupted by physical (servo)actuation saturation type limits and input delays due to the pilot actions. This results in specific nonlinear stability problems, treated with specific tools, such as describing function [18], Popov and circle criteria [5], semi-global stability [19], etc. Attempts to describe the behavior of the human pilot in the loop are given in [20], in frequency domain, and in [21], [22], in the time domain of the optimal control.

Undoubtedly, to have at hand a mathematical model of pilot behavior is very important for deriving a PIO prognostic theory. A recent work [23] describes the main steps of deriving a complex model of human pilot, based on time delay synthesis. Starting from the optimal model of the 1970s ([24], [25]), the pilot model problem is defined and solved by making reference to the control separation and duality principles and a closed-form expression of the solution is obtained.

Another paper, [26], focuses on the investigating the susceptibility of the tandem pilot-aircraft system to PIO generated by the actuator rate saturation. Both position and rate saturations in the plant model were considered in [27], by adapting the semi global stabilization theory for systems subject to input saturation [28]. So, in the two cited works [26], [27], the saturation and the delay, as possible sources of instability, are a separately approached.

This paper addresses the absolute stability problem of the pilot-aircraft system considering both the rate saturation of the actuator and the time delay in control input. A stable behavior of the closed loop pilot-aircraft system with input delay was previously obtained [23]. A short presentation of these results is given in Section 2. The problem is now if this stability survives in the presence of the actuator rate saturation. The mathematical tools of stability analysis are those of the Integral Quadratic Constraints (IQC) methodology. More specifically, the basic IQC theorem given in [8] is used as a general framework for robustness analysis of linear dynamical system pilot-aircraft with respect to uncertainties or nonlinearities defined by rate saturation and input delay.

2. A SUMMARY OF PILOT MODELING BASED ON TIME DELAY SYNTHESIS

The block diagram for the pilot-aircraft system is shown in Fig. 1. The aircraft dynamics are written in the form of a linear time invariant system [21]-[27]

$$\dot{\boldsymbol{x}}(t)=\boldsymbol{A}\boldsymbol{x}(t)+\boldsymbol{B}\delta(t)+\boldsymbol{E}w(t),\ \boldsymbol{y_o}(t)=\boldsymbol{C}\boldsymbol{x}(t)+\boldsymbol{v_y}(t):=\boldsymbol{y}(t)+\boldsymbol{v_y}(t),\ \boldsymbol{x}(0)=\boldsymbol{x}_0 \tag{1}$$

$\boldsymbol{x}(t)\in R^n$ is the state vector, $\boldsymbol{y}(t)\in R^m$ is the observation process, $\delta(t)$ is a scalar input defining the pilot command to aircraft, $w(t)$ and $\boldsymbol{v_y}(t)$ are independent Gaussian noises with intensities W, $\mathrm{diag}\left(V_{y_i}\right)$, respectively. The initial condition $\boldsymbol{x}_0\in R^n$ is a Gaussian vector such that $\boldsymbol{x}_0, w(t)$ and $\boldsymbol{v_y}(t)$ are independent. All the matrices are of appropriate dimensions. The core problem is that the human pilot inherently delays in the control loop of the aircraft. Our approach of the pilot command $\delta(t)$ modeling as a control law synthesis is based on the hypothesis that "the pilot behaves optimally" [21]-[27]. Thus, the pilot action is seen as: a) an observation component, b) a "mental" component, analogous to a Linear Quadratic Gaussian (LQG) controller, c) a decisional, "central nervous" component analogous to a dynamic predictor and d) an actuating, neuromuscular component.

Assumption 2.1. *As it was done in* [23], *the total inherent delay* 2τ *of the pilot input* δ *is shared, for convenience, into the* τ *component for observation and* τ *effective CN decision feedback component (Fig. 2).*

In the paper [23], our approach was to eliminate the Padé approximations of the central nervous block frequently used in the literature and to assume the natural representation of the time delay in control input (Fig. 2)

$$u_p(t)=u_c(t-\tau) \tag{2}$$

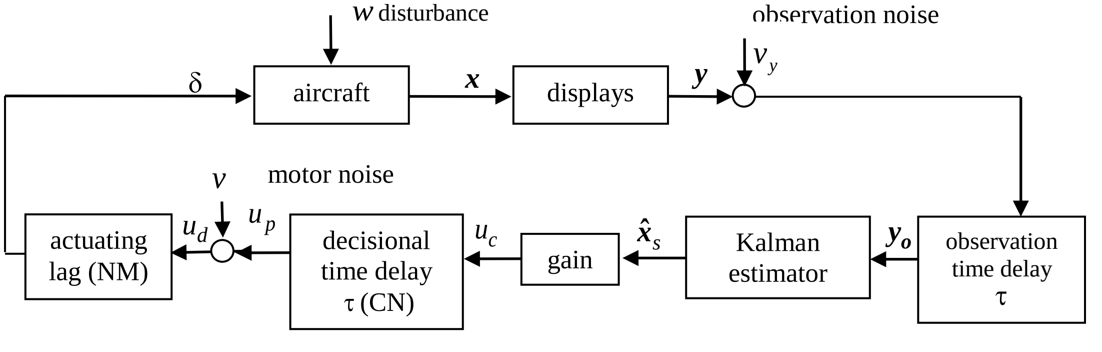

Fig. 2 – Conceptual block diagram for the pilot-vehicle system (see (12a))

Further on, the actuating neuromuscular block is modeled, as usually [23]-[25], by the lag block

$$\dot{\delta}(t)=-\delta(t)/\tau_\eta+u_d(t-\tau)/\tau_\eta,\ \delta(t)=0,\ \text{for } 0\le t\le\tau;\ u_d(t):=u_p(t)+v_u(t) \tag{3}$$

(τ_η is the neuromuscular − NM − lag and $v_u(t)$ is a Gaussian noise with intensity V_u) and by virtue of the synthesis method will be intermediary considered as part of the plant dynamics (1). Thus, the two blocks (1) and (3), in state space form, will be given by the system

$$\begin{bmatrix}\dot{\boldsymbol{x}}(t)\\ \dot{\delta}(t)\end{bmatrix}=\begin{bmatrix}\boldsymbol{A} & \boldsymbol{B}\\ 0 & -1/\tau_\eta\end{bmatrix}\begin{bmatrix}\boldsymbol{x}(t)\\ \delta(t)\end{bmatrix}+\begin{bmatrix}0\\ 1/\tau_\eta\end{bmatrix}u_c(t-\tau)+\begin{bmatrix}\boldsymbol{E} & 0\\ 0 & 1/\tau_\eta\end{bmatrix}\begin{bmatrix}\boldsymbol{w}(t)\\ v_u(t-\tau)\end{bmatrix}$$
$$\boldsymbol{y_o}(t)=[\boldsymbol{C}\quad 0]\begin{bmatrix}\boldsymbol{x}(t-\tau)\\ \delta(t-\tau)\end{bmatrix}+\boldsymbol{v}_y(t-\tau):=\boldsymbol{y}(t-\tau)+\boldsymbol{v_y}(t-\tau) \tag{4}$$

or, in matrix form, with deductible notations (e.g., $x_s:=\begin{bmatrix}x^{\mathrm{T}} & \delta\end{bmatrix}^{\mathrm{T}}$)

$$\dot{\boldsymbol{x}}_s(t)=\boldsymbol{A_s}\boldsymbol{x}_s(t)+\boldsymbol{B}_s u(t-\tau)+\boldsymbol{E_s}\boldsymbol{w}_1(t;\tau)$$
$$\boldsymbol{y_o}(t)=\boldsymbol{C_s}\boldsymbol{x_s}(t-\tau)+\boldsymbol{v}_y(t-\tau),\ \boldsymbol{x_s}(r)=0, r\in[-\tau,0] \tag{4a}$$

Remark 2.1. $\boldsymbol{w}_1$ and $\boldsymbol{v}_y$ are zero mean *stationary* Gaussian white noises with strictly positive intensities $\mathrm{diag}(W,V_u)$, $\mathrm{diag}(V_{y_i})$. Worthy to note, the variance is independent of time: $\mathrm{var}\nu_u(t-\tau)=\mathrm{var}\nu_u(t)=V_u$. For the sake of notation simplicity, $u(t-\tau):=u_p(t)=u_c(t-\tau)$.

Pilot OCM as a Linear Quadratic Gaussian (LQG) paradigm. *Given the system (4a), find the control $u(t)$ that minimizes the cost*

$$\min J(u),\quad J(u)=\lim \mathrm{E}\left(\int_0^{t_f}\left(\boldsymbol{x_s^{\mathrm{T}}}\boldsymbol{C_s^{\mathrm{T}}}\boldsymbol{Q_J}\boldsymbol{C}_s\boldsymbol{x_s}+u^2R_J\right)dt+\boldsymbol{x_s^{\mathrm{T}}}(t_f)\boldsymbol{P_f}\boldsymbol{x}_s(t_f)\right)\Big/(2t_f),\ \text{for}\ t_f\to\infty \tag{5}$$

The symbol $\mathrm{E}[f(x)]$ means the expectation of the function f of a random variable x. $\boldsymbol{Q}:=\boldsymbol{C_s^T}\boldsymbol{Q_J}\boldsymbol{C_s}\ge 0$, $R_J>0$ and $\boldsymbol{P}_f\ge 0$ weight the state vector $\boldsymbol{x}_s(t)$, the control $u(t)$ and $\boldsymbol{x}_s(t_f)$, respectively. $\boldsymbol{a}^{\mathrm{T}}$ denotes the transpose to a vector (matrix) $\boldsymbol{a}$.

Based on the separation principle and the duality principle [29], [30], the solution of pilot OCM was obtained in two steps [23]. The **first step** in the synthesis of the pilot OCM was finding of the LQR solution.

LQR paradigm. *The aircraft is described by the linear system with time delay in control input*

$$\dot{\boldsymbol{x}}_s(t)=\boldsymbol{A_s}\boldsymbol{x_s}(t)+\boldsymbol{B}_s u(t-\tau),\ \boldsymbol{x_s}(r)=0, r\in[-\tau,0] \tag{4b}$$

The pilot, based on the observation output

$$\tilde{\boldsymbol{y}}_o(t)=\boldsymbol{C_s}\boldsymbol{x_s}(t-\tau) \tag{6}$$

herein considered as a performance output (the observation is "measured" on the screen), aims to minimize the index

$$\min J(u), J(u):=J(\boldsymbol{x}_s(0),u(.),0)=$$
$$\left(\int_0^{t_f}\left(\boldsymbol{x_s^{\mathrm{T}}}\boldsymbol{C_s^{\mathrm{T}}}\boldsymbol{Q_J}\boldsymbol{C}_s\boldsymbol{x}_s+u^2R_J\right)dt+\boldsymbol{x_s^{\mathrm{T}}}(t_f)\boldsymbol{P_f}\boldsymbol{x}_s(t_f)\right)\Big/2,\ \text{for}\ t_f\to\infty \tag{7}$$

Proposition 2.1. *The solution to the LQR problem for linear time invariant system (4b), (7) with input delay, in the case of infinite horizon,* $t_f \to \infty$, *is given by*

$$u^*(t-\tau) = -R_J^{-1}\boldsymbol{B}_s^{\mathrm{T}} \exp\left(-\boldsymbol{A}_s^{\mathrm{T}}\tau\right)\boldsymbol{P}\boldsymbol{x}_s(t-\tau),$$
$$\boldsymbol{A}_s^{\mathrm{T}}\boldsymbol{P} + \boldsymbol{P}\boldsymbol{A}_s - \boldsymbol{P}\exp(-\boldsymbol{A}_s\tau)\boldsymbol{B}_s R_J^{-1}\boldsymbol{B}_s^{\mathrm{T}}\exp\left(-\boldsymbol{A}_s^{\mathrm{T}}\tau\right)\boldsymbol{P} + \boldsymbol{Q} = 0 \tag{8}$$

Proof. See [23]. The time delay synthesis machinery developed in [31] was used.

The second step in the synthesis of the optimal pilot model consisted in the statement and the solution of the estimation problem in the context of the system with time delay in the output equation

$$\boldsymbol{y}_o(t) = \boldsymbol{C}_s\boldsymbol{x}_s(t-\tau) + v_y(t-\tau) \tag{6a}$$

So, let us consider the random process $\left(\boldsymbol{x}_s(t), \boldsymbol{y}_o(t)\right)$ described by the equations (4a) with the initial condition $\boldsymbol{x}_s(r) = \varphi(r), r \in [-\tau, 0]$ given by a stochastic process, and with φ, w_1, v_y independent white noise stochastic processes.

Estimation paradigm. *Based on the observation process* $\boldsymbol{Y}(t) = \left\{\boldsymbol{y}_o(s), 0 \le s \le t\right\}$, *find the optimal estimate* $\hat{\boldsymbol{x}}_s(t)$ *of the state* $\boldsymbol{x}_s(t)$, *which minimizes the Euclidean 2-norm*

$$J = \mathrm{E}\left[\left(\boldsymbol{x}_s(t) - \hat{\boldsymbol{x}}_s(t)\right)^{\mathrm{T}}\left(\boldsymbol{x}_s(t) - \hat{\boldsymbol{x}}_s(t)\right)\middle\| \boldsymbol{F}_t^Y\right] \tag{9}$$

at every time moment t.

The operator $\mathrm{E}\left[\bullet \| \circ\right]$ in (9) means the conditional expectation of the stochastic process $\bullet$ with respect to the $\sigma-$algebra $\circ$ generated by the observation process $\boldsymbol{Y}(t) = \left\{\boldsymbol{y}_o(s), 0 \le s \le t\right\}$ [31]. A well-known result [32] is expressed by

Proposition 2.2. *The optimal estimate is given by the conditional expectation*

$$\hat{\boldsymbol{x}}_s(t) = \mathrm{E}\left[\boldsymbol{x}_s(t) \middle\| \boldsymbol{F}_t^Y\right] \tag{10}$$

The matrix function

$$\tilde{\boldsymbol{S}}(t) = \mathrm{E}\left[\left(\boldsymbol{x}_s(t) - \hat{\boldsymbol{x}}_s(t)\right)^{\mathrm{T}}\left(\boldsymbol{x}_s(t) - \hat{\boldsymbol{x}}_s(t)\right)\middle\| \boldsymbol{F}_t^Y\right] \tag{11}$$

is the estimation error variance.

Further is shown the LQG solution to both LQR problem and estimation problem.

Proposition 2.3. *The solution to the LQG problem (4a), (5) is given by the following system of equations*

$$u^*(t-\tau) = -R_J^{-1}\boldsymbol{B}_s^{\mathrm{T}}\exp\left(-\boldsymbol{A}_s^{\mathrm{T}}\tau\right)\boldsymbol{P}\hat{\boldsymbol{x}}_s(t-\tau) := \boldsymbol{K}_R\hat{\boldsymbol{x}}_s(t-\tau)$$
$$\boldsymbol{A}_s^{\mathrm{T}}\boldsymbol{P} + \boldsymbol{P}\boldsymbol{A}_s - \boldsymbol{P}\exp(-\boldsymbol{A}_s\tau)\boldsymbol{B}_s R_J^{-1}\boldsymbol{B}_s^{\mathrm{T}}\exp\left(-\boldsymbol{A}_s^{\mathrm{T}}\tau\right)\boldsymbol{P} + \boldsymbol{Q} = 0$$
$$\dot{\hat{\boldsymbol{x}}}_s(t) = \boldsymbol{A}_s\hat{\boldsymbol{x}}_s(t) + \boldsymbol{B}_s u^*(t-\tau) + \boldsymbol{K}_f\left(\boldsymbol{y}_o(t) - \boldsymbol{C}_s\hat{\boldsymbol{x}}_s(t-\tau)\right), \boldsymbol{K}_f := \boldsymbol{S}\exp\left(-\boldsymbol{A}_s^{\mathrm{T}}\tau\right)\boldsymbol{C}_s^{\mathrm{T}}\boldsymbol{V}_y^{-1} \tag{12}$$
$$\boldsymbol{S}\boldsymbol{A}_s^{\mathrm{T}} + \boldsymbol{A}_s\boldsymbol{S} + \boldsymbol{E}_s\boldsymbol{W}_1\boldsymbol{E}_s^{\mathrm{T}} - \boldsymbol{S}\exp\left(-\boldsymbol{A}_s^{\mathrm{T}}\tau\right)\boldsymbol{C}_s^{\mathrm{T}}\boldsymbol{V}_y^{-1}\boldsymbol{C}_s\exp(-\boldsymbol{A}_s\tau)\boldsymbol{S} = 0$$

Proof. See [23].

Remark 2.2. Extending classical results [29], [30], the existence of the solutions of the Riccati equations in (12) is guaranteed if the pairs $\left(\exp(-\boldsymbol{A}_s\tau)\boldsymbol{A}_s, \boldsymbol{B}_s\right)$ and $\left(\boldsymbol{A}_s, \boldsymbol{E}_s\sqrt{\boldsymbol{W}_1}\right)$ are stabilizable and the pairs $\left(\boldsymbol{C}_s, \boldsymbol{A}_s\right)$ and $\left(\boldsymbol{C}_s\exp(-\boldsymbol{A}_s\tau), \boldsymbol{A}_s\right)$ are detectable.

Corollary 2.1. *The state space representation of the pilot is given by*

$$\begin{gathered}
\boldsymbol{y}_o(t) \to \delta(t), \delta(t) = 0, \text{ for } 0 \le t \le \tau \\
\dot{\delta}(t) = -\delta(t)/\tau_\eta + u(t-\tau)/\tau_\eta, u(t-\tau) = \boldsymbol{K}_R\hat{\boldsymbol{x}}_s(t-\tau) \\
\dot{\hat{\boldsymbol{x}}}_s(t) = \boldsymbol{A}_s\hat{\boldsymbol{x}}_s(t) + \boldsymbol{B}_s u(t-\tau) + \boldsymbol{K}_f\left(\boldsymbol{y}_o(t) - \boldsymbol{C}_s\hat{\boldsymbol{x}}_s(t-\tau)\right) \\
\boldsymbol{y}_o(t) = \boldsymbol{C}_s\boldsymbol{x}_s(t-\tau) + v_y(t-\tau)
\end{gathered} \tag{12a}$$

Accordingly, the closed loop pilot-vehicle system is the following

$$\begin{gathered}
\begin{bmatrix} \dot{\boldsymbol{x}}_s(t) \\ \dot{\hat{\boldsymbol{x}}}_s(t) \end{bmatrix} = \begin{bmatrix} \boldsymbol{A}_s & 0 \\ 0 & \boldsymbol{A}_s \end{bmatrix}\begin{bmatrix} \boldsymbol{x}_s(t) \\ \hat{\boldsymbol{x}}_s(t) \end{bmatrix} + \begin{bmatrix} 0 & \boldsymbol{B}_s\boldsymbol{K}_R \\ \boldsymbol{K}_f\boldsymbol{C}_s & \boldsymbol{B}_s\boldsymbol{K}_R - \boldsymbol{K}_f\boldsymbol{C}_s \end{bmatrix}\begin{bmatrix} \boldsymbol{x}_s(t-\tau) \\ \hat{\boldsymbol{x}}_s(t-\tau) \end{bmatrix} + \\
\begin{bmatrix} \boldsymbol{E}_s \\ 0 \end{bmatrix}\boldsymbol{w}_1(t) + \begin{bmatrix} 0 \\ \boldsymbol{K}_f \end{bmatrix}\boldsymbol{v}_y(t-\tau)
\end{gathered} \tag{13}$$

or, in matrix form, and, for convenience, with zero initial condition

$$\begin{gathered}
\dot{\boldsymbol{X}}_s(t) = \boldsymbol{A}_{cl}\boldsymbol{X}_s(t) + \boldsymbol{A}_{cl\tau}\boldsymbol{X}_s(t-\tau) + \tilde{\boldsymbol{E}}_s\boldsymbol{w}_1(t) + \tilde{\boldsymbol{K}}_f\boldsymbol{v}_y(t-\tau), \boldsymbol{X}_s(t) = 0 \text{ for } -\tau \le t \le 0 \\
\boldsymbol{A}_{cl} := \begin{bmatrix} \boldsymbol{A}_s & 0 \\ 0 & \boldsymbol{A}_s \end{bmatrix}, \boldsymbol{A}_{cl\tau} := \begin{bmatrix} 0 & \boldsymbol{B}_s\boldsymbol{K}_R \\ \boldsymbol{K}_f\boldsymbol{C}_s & \boldsymbol{B}_s\boldsymbol{K}_R - \boldsymbol{K}_f\boldsymbol{C}_s \end{bmatrix}, \tilde{\boldsymbol{E}}_s := \begin{bmatrix} \boldsymbol{E}_s \\ 0 \end{bmatrix}, \tilde{\boldsymbol{K}}_f := \begin{bmatrix} 0 \\ \boldsymbol{K}_f \end{bmatrix}
\end{gathered} \tag{13a}$$

Remark 2.3. The comment in Remark 2.1 can be extended to equation (13a). The sum of two white noises $\tilde{\boldsymbol{E}}_s\boldsymbol{w}_1(t) + \tilde{\boldsymbol{K}}_f\boldsymbol{v}_y(t-\tau)$ can be represented by an equivalent white noise process $\omega(t)$

$$\begin{gathered}
\dot{\boldsymbol{X}}_s(t) = \boldsymbol{A}_{cl}\boldsymbol{X}_s(t) + \boldsymbol{A}_{cl\tau}\boldsymbol{X}_s(t-\tau) + \omega(t), \quad \boldsymbol{X}_s(t) = 0 \text{ for } -\tau \le t \le 0 \\
\text{cov}\left[\omega(t)\omega^{\mathrm{T}}(t')\right] =: \mathrm{E}\left[\omega(t)\omega^{\mathrm{T}}(t')\right] = \left(\tilde{\boldsymbol{E}}_s \text{diag}(W, V_u)\tilde{\boldsymbol{E}}_s^{\mathrm{T}} + \tilde{\boldsymbol{K}}_f \text{diag}\left(V_{y_i}\right)\tilde{\boldsymbol{K}}_f^{\mathrm{T}}\right)\delta(t-t') =: \Omega\delta(t-t')
\end{gathered} \tag{13b}$$

Stochastic differential delay equations such as (13b) were introduced in the 1960s; see, e.g., [33], in which the existence and uniqueness of the solution were discussed. Despite efforts of many researchers over time, this field is still in its infancy [34]. For example, the stability conditions are known in the case of general stochastic differential equations without delay (see, e.g., [35]) and in the case of certain delay differential equations (see e.g. [36]); instead, major difficulties are encountered because of the combination of delay and stochastic processes.

Here it should be mentioned that under LQG performed synthesis, the autonomous equation associated to equation (13b)

$$\dot{\boldsymbol{X}}_s(t) = \boldsymbol{A}_{cl}\boldsymbol{X}_s(t) + \boldsymbol{A}_{cl\tau}\boldsymbol{X}_s(t-\tau) \tag{13c}$$

is stable. In this context, it is interesting to directly check the stability of autonomous equation base on the theorem given below.

Proposition 2.4 ([36], Chapter 1, Theorem 5.2). *If* $\alpha_0 := \max\left\{\mathrm{Re}(\lambda) : \lambda \boldsymbol{I} - \boldsymbol{A}_{cl} - \boldsymbol{A}_{cl\tau} e^{-\lambda\tau} = 0\right\}$, *then, for any* $\alpha > \alpha_0$, *there is a constant* $K = K(\alpha)$ *such that the fundamental solution* φ *satisfies the inequality* $\left|\varphi(t)\right| \le K e^{\alpha t}$ $(t \ge 0)$.

To facilitate a quickly searching, by an optimization procedure, for the selection of the *noise intensities* W, V_u, $\boldsymbol{V}_y$, *an algebraic equation for the covariance of the stationary state* vector was established in [23].

Proposition 2.5. *The covariance of the stationary state vector*

$$\boldsymbol{C}_\infty := \mathrm{E}\left\{\boldsymbol{X}_s(t)\boldsymbol{X}_s^{\mathrm{T}}(t)\right\}\Big|_{t\to\infty} := \begin{bmatrix} \boldsymbol{C}_{\infty x_s} \\ \boldsymbol{C}_{\infty \hat{x}_s} \end{bmatrix} \tag{14}$$

is given by the solution of the matrix algebraic equation

$$\left(\boldsymbol{A}_{cl} + \boldsymbol{A}_{cl\tau}\varphi(-\tau)\right)\boldsymbol{C}_\infty + \boldsymbol{C}_\infty\left(\boldsymbol{A}_{cl} + \boldsymbol{A}_{cl\tau}\varphi(-\tau)\right)^{\mathrm{T}} + \Omega = 0 \tag{15}$$

The covariances of the stationary output $\boldsymbol{y}(t) = \boldsymbol{C}_s \boldsymbol{x}_s(t-\tau)$ *and control* $u(t-\tau) = \boldsymbol{K}_R \hat{\boldsymbol{x}}_s(t-\tau)$ *are described by the following relations*

$$\begin{gathered} \boldsymbol{C}_y := \mathrm{E}\left\{y(t)y^{\mathrm{T}}(t)\right\}\Big|_{t\to\infty} = \tilde{\boldsymbol{C}}_s \boldsymbol{C}_\infty \tilde{\boldsymbol{C}}_s^{\mathrm{T}} \\ \boldsymbol{C}_u := \mathrm{E}\left\{u(t)u^{\mathrm{T}}(t)\right\}\Big|_{t\to\infty} = \boldsymbol{K}_R \boldsymbol{C}_{\infty\hat{x}} \boldsymbol{K}_R^{\mathrm{T}},\ \boldsymbol{K}_R := \boldsymbol{R}_J^{-1}\boldsymbol{B}_s^{\mathrm{T}} \exp\left(-\boldsymbol{A}_s^{\mathrm{T}}\tau\right)\boldsymbol{P} \end{gathered} \tag{16}$$

In general, the control signal $\delta(t)$ is applied to a servo actuator. Herein, this is the so-called "power control unit", usually a hydraulic servo actuator installed in the command chain of the flight controls (Fig. 3). However, it should be noted that the above synthesis of the pilot model was made without considering the servo actuator dynamics. This simplification is quite common [24], [25] and can be motivated given that the actuator's dynamics are anyway much faster than the plant dynamics. This does not exclude strongly nonlinear saturation phenomena during operation: amplitude saturation (which derive from a constructive-functional constraint), and rate saturation (which is an energy constraint, in other words, an oil flow limitation).

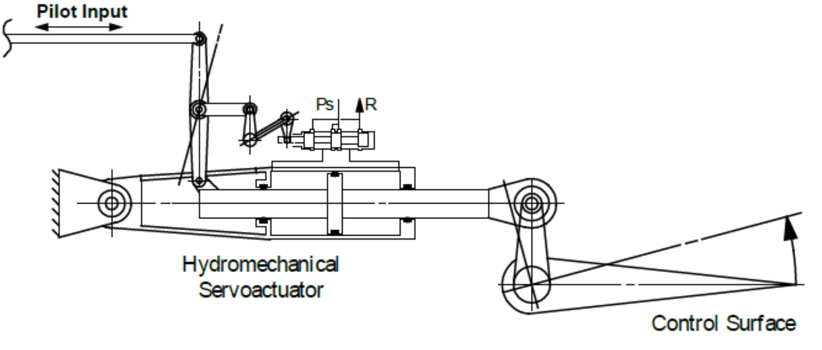

Fig. 3 – Basic scheme of flight controls with hydro-mechanical servo actuator [39]

An approach in the framework of the semi global stabilization theory for the pilot-aircraft system subject to both position and rate saturations was done in [27]. Obviously, the rate saturation modeling requires a dynamic model of the servo actuator; herein, one of first order is considered representative. Also, for reasons of simplicity, we will address the problem of absolute stability at the simultaneous emergence of the actuator rate limit and input delay, and we will neglect the actuator position limit. In this context, the updating of mathematical model summarized in the equations (1)-(16) means simply to interpose a first order servo actuator equation between the NM block output $\delta(t)$ and the effective aircraft input $\delta_{ls}(t)$

$$\begin{gathered}\dot{\boldsymbol{x}}(t)=\boldsymbol{A}\boldsymbol{x}(t)+\boldsymbol{B}\delta_{ls}(t)+\boldsymbol{E}w(t), \dot{\delta}_{ls}(t)+\omega_B\delta_{ls}(t)=\omega_B\delta(t)\\ \dot{\delta}(t)=\left(-\delta(t)+\boldsymbol{K}_R\left(\hat{\boldsymbol{x}}_s(t-\tau)\right)\right)/\tau_\eta+1/\tau_\eta v_u(t-\tau)\end{gathered} \tag{17}$$

The notation ω_B stands for the servo actuator bandwidth angular frequency, i. e., the inverse of the time constant of the hydraulic servo actuator [37], [38]. Thus, the synthesis procedure described by the equations (1)-(16) has to be step by step performed for the aircraft extended with the state δ_{ls} of a linear servo actuator

$$\begin{gathered}\dot{\boldsymbol{x}}_e(t)=\boldsymbol{A}_e\boldsymbol{x}_e(t)+\boldsymbol{B}_e\delta(t)+\boldsymbol{E}_e\boldsymbol{w}(t), \boldsymbol{x}_e=\begin{bmatrix}\boldsymbol{x}^{\mathrm{T}} & \delta_{ls}\end{bmatrix}^{\mathrm{T}}\\ \boldsymbol{A}_e=\begin{bmatrix}\boldsymbol{A} & \boldsymbol{B}\\ 0 & -\omega_B\end{bmatrix}, \boldsymbol{B}_e=\begin{bmatrix}0\\ \omega_B\end{bmatrix}, \boldsymbol{E}_e=\begin{bmatrix}\boldsymbol{E}\\ 0\end{bmatrix}\\ \dot{\delta}(t)=\left(-\delta(t)+\boldsymbol{K}_R\left(\hat{\boldsymbol{x}}_s(t-\tau)\right)\right)/\tau_\eta+v_u(t-\tau)/\tau_\eta\\ \dot{\hat{\boldsymbol{x}}}_s(t)=\boldsymbol{A}_s\hat{\boldsymbol{x}}_s(t)+\boldsymbol{B}_s\boldsymbol{K}_R\left(\hat{\boldsymbol{x}}_s(t-\tau)\right)+\boldsymbol{K}_f\left(\boldsymbol{y}_o(t)-\boldsymbol{C}_s\hat{\boldsymbol{x}}_s(t-\tau)\right)\\ \boldsymbol{x}_s=\begin{bmatrix}\boldsymbol{x}_e\\ \delta\end{bmatrix}, \boldsymbol{A}_s=\begin{bmatrix}\boldsymbol{A}_e & \boldsymbol{B}_e\\ 0 & -1/\tau_\eta\end{bmatrix}, \boldsymbol{B}_s=\begin{bmatrix}0\\ 1/\tau_\eta\end{bmatrix}, \boldsymbol{C}_s=\begin{bmatrix}\boldsymbol{C} & 0 & 0\end{bmatrix}\end{gathered} \tag{18}$$

In the above equations, the noises have been evaded for the simplicity of notation.

Numerical evaluation of pilot synthesis proposed above follows exactly the line described in [23]. The mathematical model concerns the hovering control of a VTOL-type aircraft [24]. With reference to Fig. 2, the aircraft model and the displayed outputs for the experiment deployment were

$$\dot{\boldsymbol{x}}=\begin{bmatrix}\dot{u}_g\\ \dot{U}\\ \dot{x}_h\\ \dot{q}\\ \dot{\theta}\end{bmatrix}=\begin{bmatrix}-\omega_{u_g} & 0 & 0 & 0 & 0\\ X_u & X_u & 0 & 0 & -g\\ 0 & 1 & 0 & 0 & 0\\ M_u & M_u & 0 & M_q & 0\\ 0 & 0 & 0 & 1 & 0\end{bmatrix}\begin{bmatrix}u_g\\ U\\ x_h\\ q\\ \theta\end{bmatrix}+\begin{bmatrix}0\\ 0\\ 0\\ M_\delta\\ 0\end{bmatrix}\delta+\begin{bmatrix}1\\ 0\\ 0\\ 0\\ 0\end{bmatrix}w:=\boldsymbol{A}\boldsymbol{x}+\boldsymbol{B}\delta+\boldsymbol{E}w \tag{19}$$

$$\boldsymbol{y}=\begin{bmatrix}U\\ x_h\\ q\\ \theta\end{bmatrix}=\begin{bmatrix}0 & 1 & 0 & 0 & 0\\ 0 & 0 & 1 & 0 & 0\\ 0 & 0 & 0 & 1 & 0\\ 0 & 0 & 0 & 0 & 1\end{bmatrix}\begin{bmatrix}u_g\\ U\\ x_h\\ q\\ \theta\end{bmatrix}:=\boldsymbol{C}\boldsymbol{x} \tag{20}$$

where u_g − longitudinal component of the gust velocity [m/sec]; U − velocity perturbation $\dot{x}_h$ along the aircraft x axis [m/sec]; θ − pitch attitude [rad]; $q=\dot{\theta}$ − pitch rate [rad/sec]; x_h − position [m]; δ − control stick input [mm]; M_u − speed stability parameter (0.068 rad/m/sec); M_q − pitch rate damping ($-3\ 1/\text{sec}$); M_δ − control sensitivity (0.017 rad/sec^2/mm); X_u − longitudinal drag parameter ($-0.1\ 1/\text{sec}$; g − gravitational constant, 9.81 m/sec^2; U and q are the first derivatives of x_h, and θ, respectively; ω_{u_g} − white noise filter pole (0.314 rad/sec); $\tau_\eta = 0.1\,\text{sec}$, $2\tau = 0.15\,\text{sec}$; $V_u = \pi\times 0.003\times\sigma_u^2$ and $V_{y_i} = \pi\times 0.01\times\sigma_{y_i}^2$, which correspond to normalized control noise and normalized observation noise of −25 dB and −20 dB, respectively (all the observation noise were set equal). The values of M_u, M_δ and X_u correspond to a "nominal" operating point [24]. The choice for weighting matrix Q_J was made accordingly to reference [24], $Q_J = \text{diag}\left(0\text{s}^2\text{m}^{-2}\quad 1\text{m}^{-2}\quad 37\text{s}^2\text{rad}^{-2}\quad 0\,\text{rad}^{-2}\right)$. The idea is that the task of the pilots in experiment was to minimize the hovering error. A trade between hovering error and pitch attitude error, based on measurements, is involved.

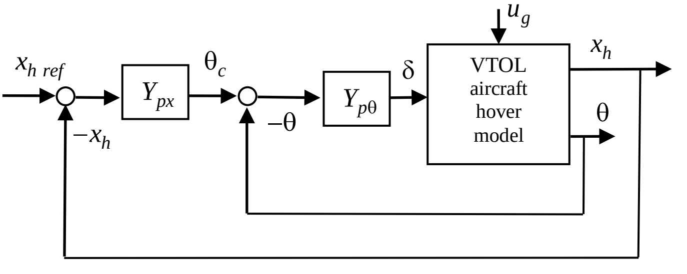

Fig. 4 – Series loop model for pilot longitudinal control in hover [24]

The determination of the matrices in the system (12a), (18) (see details in [23]) requires a systematic procedure for the selection of the noise intensities $\left(V_u, V_{y_i}\right)$ in order to obtain the above normalized observation noises. An assumption was made concerning a multiloop-model approach and an a priori closed-loop system structure illustrated in Fig. 4. In an attempt to correlate this multi-loop structure with the pilot model, the transfers functions Y_{p_x} and Y_{p_θ} must be computed

$$\begin{gathered}\delta(s) = \boldsymbol{Hy} = H_1(s)U(s) + H_2(s)x_h(s) + H_3(s)q(s) + H_4(s)\theta(s) \\ = \left(sH_1(s)+H_2(s)\right)x_h(s) + \left(sH_3(s)+H_4(s)\right)\theta(s) = -Y_{p_\theta}(s)\left(\theta(s) + Y_{p_x}(s)x_h(s)\right) \\ Y_{p_\theta}(s) := -\left(sH_3(s)+H_4(s)\right), Y_{p_x}(s) := \left(sH_1(s)+H_2(s)\right)/\left(sH_3(s)+H_4(s)\right)\end{gathered} \tag{21}$$

Human performance is predicted and compared with data obtained from *simulation experiments* in which skilled pilots executed the task. The results in [24] showed that the described there pilot model, called optimal control model (OCM) indeed reproduces most of the essential control characteristics of the pilots as well as closed-loop system performance. Numerical results shown in Fig. 5, in the form of transfer functions Y_{p_x} and Y_{p_θ}, represent a comparison of experimental results reported in [40], [41] with theoretical results described by the system (12a), (18). The following transfer function associated to (12a)

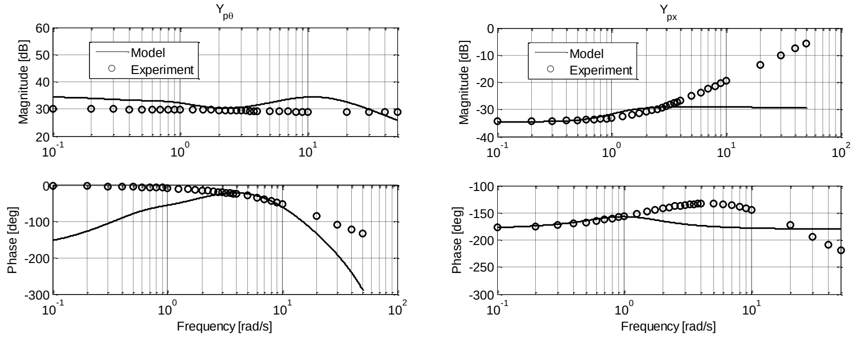

a) transfer function Y_{p_θ} ; b) transfer function Y_{p_x}

Fig. 5 – Comparison of experimental and theoretical results involving the transfer functions Y_{p_x} and Y_{p_θ} . “Experiment” means “experimental data obtained with skilled pilots”; “model” means “numerical simulations on the system (12a), (18)”

$$\frac{\delta(s)}{\boldsymbol{y}(s)}=\frac{e^{-2\tau s}\boldsymbol{K_R}}{\tau_\eta s+1}\left(s\boldsymbol{I}-\boldsymbol{A_s}-\boldsymbol{B_s K_R}+\boldsymbol{K_f C_s}\right)^{-1}\boldsymbol{K_f} \tag{22}$$

was considered as a mathematical “model” in numerical evaluations (Fig. 5). The increased phase shift with respect to experimental values is consistent with the framework of the delay synthesis. However, under conditions specified in Remark 2.2, the closed loop system (13), even with the extensions in (18), is designed as stable. The question arises if the dynamical stability is preserved in the presence of rate saturation.

Compared to the previous equations (18), the occurrence of the rate saturation is modeled as follows

$$\begin{gathered}
\dot{\boldsymbol{x}}(t)=\boldsymbol{A x}(t)+\boldsymbol{B}\delta_{ns}(t)+\boldsymbol{E w}(t), \dot{\delta}_{ns}(t)=\operatorname{sat}\left(\omega_{\mathrm{B}}\left(\delta(t)-\delta_{ns}(t)\right)\right) \\
\dot{\delta}(t)=\left(-\delta(t)+\boldsymbol{K}_R\left(\hat{\boldsymbol{x}}_s(t-\tau)\right)\right)/\tau_\eta+v_u(t-\tau)/\tau_\eta, \boldsymbol{y}_o(t)=\boldsymbol{C_s x_s}(t-\tau)+v_y(t-\tau) \\
\dot{\hat{\boldsymbol{x}}}_s(t)=\boldsymbol{A}_s\hat{\boldsymbol{x}}_s(t)+\boldsymbol{B}_s\boldsymbol{K}_R\left(\hat{\boldsymbol{x}}_s(t-\tau)\right)+\boldsymbol{K}_f\left(\boldsymbol{y}_o(t)-\boldsymbol{C}_s\hat{\boldsymbol{x}}_s(t-\tau)\right) \\
\boldsymbol{x}_s=\begin{bmatrix}\boldsymbol{x}\\ \delta_{ns}\\ \delta\end{bmatrix}, \boldsymbol{A}_s=\begin{bmatrix}\boldsymbol{A} & \boldsymbol{B} & 0\\ 0 & -\omega_{\mathrm{B}} & \omega_{\mathrm{B}}\\ 0 & 0 & -1/\tau_\eta\end{bmatrix}, \boldsymbol{B}_s=\begin{bmatrix}0\\ 0\\ 1/\tau_\eta\end{bmatrix}, \boldsymbol{C}_s=\begin{bmatrix}\boldsymbol{C} & 0 & 0\end{bmatrix}
\end{gathered} \tag{23}$$

A typical block diagram of the rate saturation, also called *rate limiter* [42], is shown in Fig. 6. This diagram describes the simplified and established servo actuator model with rate saturation [16], [26], [27], [37] (an easily different scheme is proposed in [42]). Saturation occurs when the error signal e exceeds the saturation value, $e_L=V_L/\omega_B$. During saturation, the output δ_{ns} is required to move at its maximum rate V_L until error signal reduced.

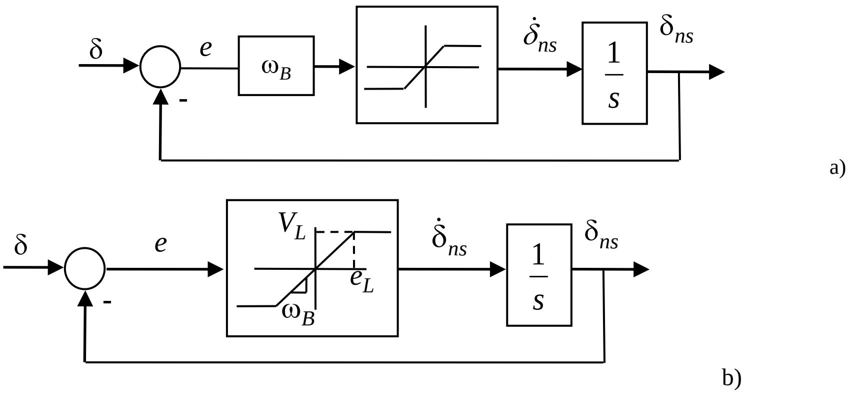

Fig. 6 − a) Block diagram of the rate limiter; b) equivalent scheme

3. SOME FUNDAMENTALS OF IQC-BASED STABILITY ANALYSIS

The IQC framework for the absolute stability analysis allows the expression of many absolute stability criteria (Popov criterion, circle criterion [5], other criteria, e.g., [44]) in terms of a single unifying theory [8]. The fundamental result provided in [8] will be reported below for the sake of completeness. For self-containedness, a minumum theoretical framework is clarified below. Let R be the set of real numbers and C the set of complex numbers. The set of square integrable functions on R^l is denoted by $\boldsymbol{L}_2$ and the set of functions on R^l that are square integrable on any compact set is denoted by $\boldsymbol{L}_{2e}$. $\boldsymbol{L}_2$ and $\boldsymbol{L}_{2e}$ are normed spaces. We can take as example $\boldsymbol{L}_2[0,\infty)$, the space of R^l-valued functions $\boldsymbol{f}:[0,\infty)\to R^l$ of finite energy: $\|\boldsymbol{f}\|^2 := \int_0^\infty |\boldsymbol{f}(t)|^2 \mathrm{d}t := \langle \boldsymbol{f}, \boldsymbol{f} \rangle$.

The above noted space $\boldsymbol{L}_{2e}$ is an *extended space* consisting of signals that may not be bounded in the norm of the vector space but any their truncation to a finite time interval is bounded. Extended spaces are usually defined only for time axes included in R_+, because only causal systems starting at time zero are considered. A formalized definition of the extended space highlights the truncation operator $\boldsymbol{P}_T$ which leaves a function unchanged on the interval $[0,T]$ and gives the value zero on (T,∞). The c*ausality* of an operator $\boldsymbol{F}$ means that $\boldsymbol{P}_T\boldsymbol{F} = \boldsymbol{P}_T\boldsymbol{F}\boldsymbol{P}_T$ for any $T > 0$ [8].

Consider the system in Fig. 1b, where the linear part $\boldsymbol{G}$ is a linear time-invariant operator defined by a transfer matrix $\boldsymbol{G}(s)$ and the nonlinear part is given by a bounded gain nonlinear operator $\boldsymbol{\Delta}:\boldsymbol{L}_{2e}\to\boldsymbol{L}_{2e}$. In applications, the bounded and causal operator $\boldsymbol{\Delta}$ describes the “troublemaking” [8] components of a system: the nonlinearities, delays, or uncertainties).

The positive feedback interconnection of $\boldsymbol{G}$ and $\boldsymbol{\Delta}$ is described by the relations

$$\boldsymbol{\sigma} = \boldsymbol{G}\boldsymbol{u} + \boldsymbol{\mu},\ \boldsymbol{u} = \Delta(\boldsymbol{\sigma}) + \boldsymbol{\eta} \tag{24}$$

where μ and η represent interconection noises on $\boldsymbol{L}_{2e}$ (see Fig. 1b). The dimensions of all spaces, functions and operators are appropiate, but are evaded for simplicity of notation (an operator is a mapping from a normed space into another).

It is assumed the *well-posedness* of the interconnection, i. e., the operator $(\boldsymbol{\sigma},\boldsymbol{u})\rightarrow(\boldsymbol{g},\boldsymbol{f})$ defined by (24) is *causally invertible*. The well-posedness is equivalent to the existence, uniqueness and continuity of the solutions of the underlying differential equations [8]. The interconnection is *stable* if, in addition, the *inverse is bounded*, i. e., if there exists a constant $c>0$ such that

$$\int_0^T\left(|\boldsymbol{\sigma}|^2+|\boldsymbol{u}|^2\right)\mathrm{d}t\le c\int_0^T\left(|\boldsymbol{\mu}|^2+|\boldsymbol{\eta}|^2\right)\mathrm{d}t \tag{25}$$

for any $T\ge 0$ and for any solution of (24). The *gain* of an operator $\boldsymbol{F}:\boldsymbol{L}_{2e}[0,\infty)\rightarrow\boldsymbol{L}_{2e}[0,\infty)$ is given by $\|\boldsymbol{F}\|=\sup\left\{\|\boldsymbol{F}(\boldsymbol{f})\|/\|\boldsymbol{f}\|:\boldsymbol{f}\in\boldsymbol{L}_2[0,\infty),\ \boldsymbol{f}\ne 0\right\}$. The operator is *bounded* if the gain is finite.

The IQCs are quadratic forms characterizing the structure of the operators in Hilbert spaces H , i. e., in complete normed vector spaces with norm defined in terms of an inner product. More specifically, an IQC is defined as an *self-adjoints operator* [9], whose *matrix* $\boldsymbol{M}$ *is, consequently, Hermitian,* $\boldsymbol{M}=\boldsymbol{M}^*$ (the exponent $^{(*)}$ means the transpose and conjugate applied to a complex matrix). Let $\boldsymbol{\Pi}$ a bounded and self-adjoint operator, Therefore, given $\boldsymbol{u}=\Delta(\boldsymbol{\sigma})$ (see Fig. 1b), we say that the signals $\boldsymbol{\sigma},\ \boldsymbol{u}$ satisfy the IQC defined by $\boldsymbol{\Pi}$ if (as defined by a transfer matrix, $\boldsymbol{\Pi}(j\omega)=\boldsymbol{\Pi}(j\omega)^*$)

$$Q(\sigma,\Delta(\sigma))=:\left\langle\begin{bmatrix}\boldsymbol{\sigma}\\ \boldsymbol{u}\end{bmatrix},\Pi\begin{bmatrix}\boldsymbol{\sigma}\\ \boldsymbol{u}\end{bmatrix}\right\rangle=\int_{-\infty}^{\infty}\begin{bmatrix}\boldsymbol{\sigma}(t)\\ \boldsymbol{u}(t)\end{bmatrix}^{\mathrm{T}}\boldsymbol{\Pi}\left(\begin{bmatrix}\boldsymbol{\sigma}(t)\\ \boldsymbol{u}(t)\end{bmatrix}\right)\mathrm{d}t=\int_{-\infty}^{\infty}\begin{bmatrix}\hat{\boldsymbol{\sigma}}(j\omega)\\ \hat{\boldsymbol{u}}(j\omega)\end{bmatrix}^{*}\boldsymbol{\Pi}(j\omega)\begin{bmatrix}\hat{\boldsymbol{\sigma}}(j\omega)\\ \hat{\boldsymbol{u}}(j\omega)\end{bmatrix}\mathrm{d}\omega\ge 0 \tag{26}$$

$\forall\boldsymbol{\sigma}\in\boldsymbol{L}_2[0,\infty)$. Here $\hat{\boldsymbol{\sigma}}(j\omega)$ and $\hat{\boldsymbol{u}}(j\omega)$ are Fourier transforms of the signals $\boldsymbol{\sigma},u\in\boldsymbol{L}_2[0,\infty)$. In fact, IQCs are weightings, or multipliers. In other words, the quadratic form $Q(\boldsymbol{\sigma},\Delta(\boldsymbol{\sigma}))$ keeps a constant sign, whatever the input $\boldsymbol{\sigma}\in\boldsymbol{L}_2[0,\infty)$, a Hilbert space.

The main result of the IQC-based stability analysis is given below.

Theorem 3.1 [8]. *Consider a linear system defined by a stable transfer matrix* $\boldsymbol{G}(s)$, *and a bounded causal operator* $\boldsymbol{\Delta}:\boldsymbol{L}_{2e}\rightarrow\boldsymbol{L}_{2e}$. *Assume that: 1) for every* $\tau\in[0,1]$, *the interconnection of* $\boldsymbol{G}$ *and* $\tau\boldsymbol{\Delta}$, *as defined in (24), is well-posed; 2) for every* $\tau\in[0,1]$, *the IQC (26) is satisfied by* $\tau\boldsymbol{\Delta}$ *; 3) there exists* $\varepsilon>0$ *such that*

$$\begin{bmatrix}\boldsymbol{G}(j\omega)\\ \boldsymbol{I}\end{bmatrix}^*\Pi(j\omega)\begin{bmatrix}\boldsymbol{G}(j\omega)\\ \boldsymbol{I}\end{bmatrix}\le-\varepsilon\boldsymbol{I},\quad\forall\omega\in\boldsymbol{R}. \tag{27}$$

Then, the feedback interconnection of $\boldsymbol{G}$ *and* $\boldsymbol{\Delta}$ *is stable.*

4. APPLICATION TO STABILITY ANALYSIS OF THE AIRCRAFT-PILOT SYSTEM WITH RATE SATURATION AND INPUT DELAY

Remember now the components of the aircraft-pilot system: the aircraft equation, the actuator rate saturation equation, the optimal pilot model designed in the framework of input delay theory in which we add NM lag

$$\begin{gathered}\dot{\boldsymbol{x}}(t)=\boldsymbol{A}\boldsymbol{x}(t)+\boldsymbol{B}\delta_{ns}(t)+\boldsymbol{E}\boldsymbol{w}(t),\ \dot{\delta}_{ns}(t)=\mathrm{sat}\left(\omega_{\mathrm{B}}\left(\delta(t)-\delta_{ns}(t)\right)\right)\\ \dot{\delta}(t)=-\delta(t)/\tau_\eta+\boldsymbol{K}_R\left(\hat{\boldsymbol{x}}_s(t-\tau)\right)/\tau_\eta+v_u(t-\tau)/\tau_\eta,\\ \boldsymbol{x}_s:=\begin{bmatrix}\boldsymbol{x}^{\mathrm{T}} & \delta_{ns} & \delta\end{bmatrix}^{\mathrm{T}}\\ \dot{\hat{\boldsymbol{x}}}_s(t)=\boldsymbol{A}_s\hat{\boldsymbol{x}}_s(t)+\boldsymbol{B}_s\boldsymbol{K}_R\hat{\boldsymbol{x}}_s(t-\tau)+\boldsymbol{K}_f\left(\boldsymbol{y}_o(t)-\boldsymbol{C}_s\hat{\boldsymbol{x}}_s(t-\tau)\right)\\ \boldsymbol{y}_o(t)=\boldsymbol{C}_s\boldsymbol{x}_s(t-\tau)+v_y(t-\tau)\\ \boldsymbol{A}_s=\begin{bmatrix}\boldsymbol{A}_e & \boldsymbol{B}_e\\ 0 & -1/\tau_\eta\end{bmatrix},\ \boldsymbol{B}_s=\begin{bmatrix}0\\ 1/\tau_\eta\end{bmatrix},\boldsymbol{C}_s=\begin{bmatrix}\boldsymbol{C} & 0 & 0\end{bmatrix}\\ \boldsymbol{A}_e=\begin{bmatrix}\boldsymbol{A} & \boldsymbol{B}\\ 0 & -\omega_B\end{bmatrix},\ \boldsymbol{B}_e=\begin{bmatrix}0\\ \omega_B\end{bmatrix},\boldsymbol{E}_e=\begin{bmatrix}\boldsymbol{E}\\ 0\end{bmatrix}\end{gathered} \tag{28}$$

We choose the vector signals $\boldsymbol{u}$ and $\boldsymbol{\sigma}$ as follows

$$\begin{gathered}\sigma_1(t):=\delta(t),\boldsymbol{\sigma}_2(t):=\boldsymbol{x}_s(t),\boldsymbol{\sigma}_3(t):=\hat{\boldsymbol{x}}_s(t)\\ u_1(t)=\mathrm{sat}\left(\omega_B\left(\sigma_1-\delta_{ns}(t)\right)\right),\ \boldsymbol{u}_2(t)=\boldsymbol{x}_s(t-\boldsymbol{\tau})-\boldsymbol{x}_s(t),\ \boldsymbol{u}_3(t)=\hat{\boldsymbol{x}}_s(t-\boldsymbol{\tau})-\hat{\boldsymbol{x}}_s(t)\end{gathered} \tag{29}$$

The next step is to find a linear part of the system (28), (29). Given the new variables (29), we rewrite the system (28) by ignoring the noises, which anyway are intercepted in the structure of Fig. 1b

$$\begin{gathered}\dot{\boldsymbol{x}}(t)=\boldsymbol{A}\boldsymbol{x}(t)+\boldsymbol{B}\delta_{ns}(t),\ \dot{\delta}_{ns}(t)=u_1(\delta;\omega_B),\dot{\delta}(t)=-\delta(t)/\tau_\eta+\boldsymbol{K}_R\left(\boldsymbol{u}_3(t)+\hat{\boldsymbol{x}}_s(t)\right)/\tau_\eta\\ \dot{\hat{\boldsymbol{x}}}_s(t)=\boldsymbol{K}_f\boldsymbol{C}_s\boldsymbol{x}_s(t)+\left(\boldsymbol{A}_s+\boldsymbol{B}_s\boldsymbol{K}_R-\boldsymbol{K}_f\boldsymbol{C}_s\right)\hat{\boldsymbol{x}}_s(t)+\boldsymbol{K}_f\boldsymbol{C}_s\boldsymbol{u}_2(t)+\left(\boldsymbol{B}_s\boldsymbol{K}_R-\boldsymbol{K}_f\boldsymbol{C}_s\right)\boldsymbol{u}_3(t)\end{gathered} \tag{30}$$

An intermediate relationship was used

$$\begin{gathered}\boldsymbol{x}_s(t-\boldsymbol{\tau})-\hat{\boldsymbol{x}}_s(t-\boldsymbol{\tau})=\\ \boldsymbol{x}_s(t-\boldsymbol{\tau})-\boldsymbol{x}_s(t)-\hat{\boldsymbol{x}}_s(t-\boldsymbol{\tau})+\hat{\boldsymbol{x}}_s(t)+\boldsymbol{x}_s(t)-\hat{\boldsymbol{x}}_s(t)=\boldsymbol{u}_2(t)-\boldsymbol{u}_3(t)+\boldsymbol{\sigma}_2(t)-\boldsymbol{\sigma}_3(t)\end{gathered} \tag{31}$$

It is not difficult to see that the matrix associated to the system

$$\begin{gathered}\begin{bmatrix}\dot{\boldsymbol{x}}\\ \dot{\delta}_{ns}\\ \dot{\delta}\\ \dot{\hat{\boldsymbol{x}}}_s\end{bmatrix}=\begin{bmatrix}\boldsymbol{A} & \boldsymbol{B} & 0 & 0\\ 0 & 0 & 0 & 0\\ 0 & 0 & -1/\tau_\eta & \boldsymbol{K}_R/\tau_\eta\\ & \boldsymbol{K}_f\boldsymbol{C}_s & & \boldsymbol{A}_s+\boldsymbol{B}_s\boldsymbol{K}_R-\boldsymbol{K}_f\boldsymbol{C}_s\end{bmatrix}\begin{bmatrix}\boldsymbol{x}\\ \delta_{ns}\\ \delta\\ \hat{\boldsymbol{x}}_s\end{bmatrix}+\\ \begin{bmatrix}0 & 0 & 0\\ 1 & 0 & 0\\ 0 & 0 & \boldsymbol{K}_R/\tau_\eta\\ 0 & \boldsymbol{K}_f\boldsymbol{C}_s & \boldsymbol{B}_s\boldsymbol{K}_R-\boldsymbol{K}_f\boldsymbol{C}_s\end{bmatrix}\begin{bmatrix}u_1\\ \boldsymbol{u}_2\\ \boldsymbol{u}_3\end{bmatrix}\end{gathered} \tag{32}$$

is not a stable matrix, so a basic condition in Theorem 3.1 is not satisfied. At first glance, this compromises the solution of the problem in the framework of IQC paradigm. Without excluding other possible approaches, in the following we consider a technique of *encapsulation in a feedback loop* [41], [45], [46] of the pure integrator $1/s$ that we see in the second row of the relation (32). This way, the model is put in the limits of applicability of the Theorem 3.1. Performing a slight change of variables with respect to (29), in accordance with the block diagram in Fig. 7

$$\begin{gathered}\sigma_1(t) := \delta(t), \boldsymbol{\sigma}_2(t) := \boldsymbol{x}_s(t), \boldsymbol{\sigma}_3(t) := \hat{\boldsymbol{x}}_s(t) \\ u_1(t) := \mathrm{sat}\left(\omega_B\left(\sigma_1(t) - \delta_{ns}(t)\right)\right) - \boldsymbol{\omega}_B\left(\sigma_1(t) - \delta_{ns}(t)\right) \\ \boldsymbol{u}_2(t) := \boldsymbol{\sigma}_2(t-\boldsymbol{\tau}) - \boldsymbol{\sigma}_2(t), \boldsymbol{u}_3(t) := \boldsymbol{\sigma}_3(t-\boldsymbol{\tau}) - \boldsymbol{\sigma}_3(t)\end{gathered} \tag{29a}$$

we get a new form of the system

$$\begin{gathered}\begin{bmatrix}\dot{\boldsymbol{x}} \\ \dot{\delta}_{ns} \\ \dot{\delta} \\ \dot{\hat{\boldsymbol{x}}}_s\end{bmatrix} = \begin{bmatrix}\boldsymbol{A} & \boldsymbol{B} & \boldsymbol{0}_{5\times1} & \boldsymbol{0}_{5\times7} \\ \boldsymbol{0}_{1\times5} & -\boldsymbol{\omega}_B & \boldsymbol{\omega}_B & \boldsymbol{0}_{1\times7} \\ \boldsymbol{0}_{1\times5} & 0 & -1/\tau_\eta & \boldsymbol{K}_R/\tau_\eta \\ & \boldsymbol{K}_f\boldsymbol{C} & & \boldsymbol{A}_s + \boldsymbol{B}_s\boldsymbol{K}_R - \boldsymbol{K}_f\boldsymbol{C}_s\end{bmatrix}\begin{bmatrix}\boldsymbol{x} \\ \delta_{ns} \\ \delta \\ \hat{\boldsymbol{x}}_s\end{bmatrix} + \\ \begin{bmatrix}0 & \boldsymbol{0}_{5\times7} & \boldsymbol{0}_{5\times7} \\ 1 & \boldsymbol{0}_{1\times7} & \boldsymbol{0}_{1\times7} \\ 0 & \boldsymbol{0}_{1\times7} & \boldsymbol{K}_R/\boldsymbol{\tau}_\eta \\ 0 & \boldsymbol{K}_f\boldsymbol{C}_s & \boldsymbol{B}_s\boldsymbol{K}_R - \boldsymbol{K}_f\boldsymbol{C}_s\end{bmatrix}\begin{bmatrix}u_1 \\ \boldsymbol{u}_2 \\ \boldsymbol{u}_3\end{bmatrix}, \begin{bmatrix}\sigma_1 \\ \boldsymbol{\sigma}_2 \\ \boldsymbol{\sigma}_3\end{bmatrix} = \begin{bmatrix}\boldsymbol{0}_{1\times5} & 0 & 1 & \boldsymbol{0}_{1\times7} \\ \boldsymbol{I}_7 & & \boldsymbol{0}_{7\times7} & \\ \boldsymbol{0}_{7\times7} & & \boldsymbol{I}_7 & \end{bmatrix}_{15\times14}\begin{bmatrix}\boldsymbol{x} \\ \delta_{ns} \\ \delta \\ \hat{\boldsymbol{x}}_s\end{bmatrix} + 0\times\begin{bmatrix}u_1 \\ \boldsymbol{u}_2 \\ \boldsymbol{u}_3\end{bmatrix}\end{gathered} \tag{32a}$$

respectively

$$\begin{gathered}\dot{\boldsymbol{x}}(t) = \boldsymbol{A}\boldsymbol{x}(t) + \boldsymbol{B}\delta_{ns}(t), \dot{\delta}_{ns}(t) = \omega_B\left(\delta - \delta_{ns}(t)\right) + u_1(\delta; \omega_B) \\ \dot{\delta}(t) = -\delta(t)/\tau_\eta + \boldsymbol{K}_R\left(\boldsymbol{u}_3(t) + \hat{\boldsymbol{x}}_s(t)\right)/\tau_\eta \\ \dot{\hat{\boldsymbol{x}}}_s(t) = \boldsymbol{K}_f\boldsymbol{C}_s\boldsymbol{x}_s(t) + \left(\boldsymbol{A}_s + \boldsymbol{B}_s\boldsymbol{K}_R - \boldsymbol{K}_f\boldsymbol{C}_s\right)\hat{\boldsymbol{x}}_s(t) + \\ \boldsymbol{K}_f\boldsymbol{C}_s\boldsymbol{u}_2(t) + \left(\boldsymbol{B}_s\boldsymbol{K}_R - \boldsymbol{K}_f\boldsymbol{C}_s\right)\boldsymbol{u}_3(t)\end{gathered} \tag{32b}$$

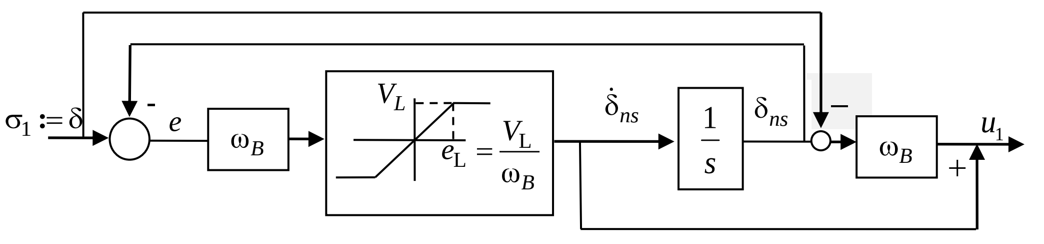

Fig.7 – Encapsulation of the rate limiter

On the one hand, analyzing the state matrix in equation (32a), we see that it is stable, moreover, this is even the state matrix that was used in the LQG synthesis with delay. On the other hand, the definitions (29a) mean the introducing of the nonlinear operator Δ (Fig. 1)

$$\boldsymbol{u} := \begin{bmatrix}u_1 \\ \boldsymbol{u}_2 \\ \boldsymbol{u}_3\end{bmatrix} = \Delta\begin{pmatrix}\sigma_1 \\ \boldsymbol{\sigma}_2 \\ \boldsymbol{\sigma}_3\end{pmatrix} := \begin{bmatrix}\Gamma_{\mathrm{sat}}^{\omega_B}(\sigma_1) \\ \boldsymbol{\sigma}_2(t-\tau) - \boldsymbol{\sigma}_2(t) \\ \boldsymbol{\sigma}_3(t-\tau) - \boldsymbol{\sigma}_3(t)\end{bmatrix} \tag{33}$$

with the operator $\Gamma_{\text{sat}}^{\omega_B}(\sigma_1)$ defined by the relations

$$u_1(t)=\dot{\delta}_{ns}(t)+\omega_B(\delta_{ns}(t)-\delta),\ \dot{\delta}_{ns}(t)=\text{sat}(\omega_B(\sigma_1-\delta_{ns}(t))),\ \delta_{ns}(0)=0 \tag{33a}$$

Let now write the linear part $\boldsymbol{G}$ of the system according to Fig. 1. With deductible notations, the system (32a) gives

$$\dot{\boldsymbol{X}}=\boldsymbol{A_G X}+\boldsymbol{B_G u},\ \boldsymbol{\sigma}=\boldsymbol{C_G X} \tag{34}$$

therefore we have defined the system matrix $\boldsymbol{G}$

$$\boldsymbol{G}(\boldsymbol{s})=\boldsymbol{C_G}(\boldsymbol{sI}-\boldsymbol{A_G})^{-1}\boldsymbol{B_G},\boldsymbol{G}(\boldsymbol{s})\in\boldsymbol{M}_{15} \tag{35}$$

Taking into account the sizes of the systems described in (18), (19), (28), (29), it follows that $\boldsymbol{G}(\boldsymbol{s})\in\boldsymbol{M}_{15}$, where by M_n is denoted the set of $n\times n$ complex matrices.

Having in mind the definition (26) of the IQC multiplier, we are interested to obtain an assessment of the gains $\boldsymbol{\sigma}_i\to\boldsymbol{u}_i$, $i=1,2,3$. For this purpose, we first get

Proposition 4.1. *The* L_2*-induced gain of the mapping*

$$\sigma_1:=\delta\to u_1:=\omega_B(\delta_{ns}-\sigma_1)+\text{sat}(\omega_B(\sigma_1-\delta_{ns}))$$

does not exceed $k_{\text{sat}}:=\max\{1,\sqrt{2}\omega_B\}+\omega_B$.

The proof adjusts the result from [45], Theorem 3.4, p. 11. The function $\Phi(z)=\text{sat}(z)$ is a semi concave function as defined in [45], with $\Phi(0)=1$, so the upper bound of the operator $\sigma_1\to u_1:=\omega_B\delta_{ns}+\text{sat}(\omega_B(\sigma_1-\delta_{ns}))$ does not exceed $\max\{1,\sqrt{2}\omega_B\}$. Therefore the upper bound refers to the operator

$$\sigma_1:=\delta\to u_1:=\omega_B\delta_{ns}+\text{sat}(\omega_B(\sigma_1-\delta_{ns}))$$

$$|u_1/\boldsymbol{\sigma}_1|=|\omega_B(\delta_{ns}-\sigma_1)+\text{sat}(\omega_B(\sigma_1-\delta_{ns}))/\sigma_1|\le$$

$$|\text{sat}(\omega_B(\sigma_1-\delta_{ns}))+\omega_B\delta_{ns}/\sigma_1|+\omega_B\le\max\{1,\sqrt{2}\boldsymbol{\omega}_B\}+\boldsymbol{\omega}_B$$

Observe that, based on the definitions

$$\text{sat}\ \omega_B(\delta-\delta_{ns})=\begin{cases}\omega_B(\delta-\delta_{ns}), & \omega_B|\delta-\delta_{ns}|<V_L=\dot{\delta}_{nsL}\\ V_L\,\text{sgn}(\delta-\delta_{ns}), & \omega_B|\delta-\delta_{ns}|\ge V_L=\dot{\delta}_{nsL}\end{cases}$$

$$\text{sat}(\delta-\delta_{ns})=\begin{cases}\delta-\delta_{ns}, & |\delta-\delta_{ns}|<e_L:=V_L/\omega_B\\ e_L\,\text{sgn}(\delta-\delta_{ns}), & |\delta-\delta_{ns}|\ge e_L\end{cases}$$

the identity $\text{sat}[\omega_B(\delta-\delta_{ns})]\equiv\omega_B\,\text{sat}(\delta-\delta_{ns})$ holds, as shown in Fig. 6.

In fact, Proposition 4.1 substantiates the following multiplier

$$\boldsymbol{\Pi}_{\sigma_1 u_1}=\begin{bmatrix}k_{\text{sat}}^2 & 0\\ 0 & -1\end{bmatrix} \tag{36}$$

Indeed, the definition of the of IQC multiplier (26) is written in this case as

$$\left\langle \begin{bmatrix} \sigma_1 \\ u_1 \end{bmatrix}, \begin{bmatrix} k_{\text{sat}}^2 & 0 \\ 0 & -1 \end{bmatrix} \begin{bmatrix} \sigma_1 \\ u_1 \end{bmatrix} \right\rangle = k_{\text{sat}}^2 \sigma_1^2 - u_1^2(\sigma_1) \ge 0 \tag{26'}$$

which just asserts Proposition 4.1. It should be added that various other IQCs of the rate limiter are proposed in literature. These IQCs transcribe a sector condition, or the Popov criterion, or the Zames-Falb multipliers [47] etc.

Proposition 4.2. *Consider an uncertain delay* $\tau \in [0,1]$. *The* L_2*-induced gain in the mappings* $\boldsymbol{\sigma}_2(t) := \boldsymbol{x}_s(t) \to \boldsymbol{u}_2(t) := \boldsymbol{x}_s(t-\boldsymbol{\tau}) - \boldsymbol{x}_s(t)$, $\boldsymbol{\sigma}_3(t) := \hat{\boldsymbol{x}}_s(t) \to \boldsymbol{u}_3(t) = \hat{\boldsymbol{x}}_s(t-\boldsymbol{\tau}) - \hat{\boldsymbol{x}}_s(t)$ *does not exceed the bound*

$$k_{\text{delay}} := \sqrt{\psi_0(\omega)} = \sqrt{\left(\omega^2 + 0.08\omega^4\right) / \left(1 + 0.13\omega^2 + 0.02\omega^4\right)} \tag{37}$$

Indeed, with $\tau \in [0,1]$, we get

$$\begin{gathered} \hat{\boldsymbol{u}}_2(j\omega) = \left(e^{-j\omega\tau} - 1\right)\hat{\boldsymbol{\sigma}}_2(j\omega) \\ \left|\hat{\boldsymbol{u}}_2(j\omega)\right|^2 = \left|e^{-j\omega\tau} - 1\right|^2 \left|\hat{\boldsymbol{\sigma}}_2(j\omega)\right|^2 = \left|\cos(\omega\tau) - j\sin(\omega\tau) - 1\right|^2 \left|\hat{\boldsymbol{\sigma}}_2(j\omega)\right|^2 = \\ \left[\cos^2(\omega\tau) + 1 - 2\cos(\omega\tau) + \sin^2(\omega\tau)\right] \left|\hat{\boldsymbol{\sigma}}_2(\omega\tau)\right|^2 = \\ 2\left[1 - \cos(\omega\tau)\right]\left|\hat{\boldsymbol{\sigma}}_2(\omega\tau)\right|^2 = 2\left[1 - \cos^2((\omega\tau)/2) + \sin^2((\omega\tau)/2)\right]\left|\hat{\boldsymbol{\sigma}}_2(\omega\tau)\right|^2 = 4\sin^2((\omega\tau)/2)\left|\hat{\boldsymbol{\sigma}}_2(j\omega)\right|^2 \end{gathered} \tag{38}$$

Define

$$\psi_*(\omega) = \max_{\tau \in [0,\tau_0]} \left| 4\sin^2\left(\frac{\tau}{\tau_0}\frac{\omega}{2}\right) \right| = \begin{cases} 4\sin^2(\omega/2), \ \omega < \pi \\ 4, \ \omega \ge \pi \end{cases} \tag{39}$$

To assessing the relative conservativeness of various absolute stability criteria, we are looking for weightings as defined in (26), thus we seek a rational upper bound of $\psi_*(\omega)$. Such a function is even $\psi_0(\omega)$ given in (37) (Fig. 8). The construction of this function relies on Propositions 2 and 3 from [48], which describe upper bounds of delay operators, with uncertain, but constant $\tau \in [0,1]$. Therefore

$$\left|\hat{\boldsymbol{u}}_2(j\omega)\right|^2 \le \psi_0(\omega)\left|\hat{\boldsymbol{\sigma}}_2(j\omega)\right|^2, \left|\hat{\boldsymbol{u}}_3(j\omega)\right|^2 \le \psi_0(\omega)\left|\hat{\boldsymbol{\sigma}}_3(j\omega)\right|^2 \tag{40}$$

This consideration ends the proof.

Proposition 4.2 substantiates the following multipliers

$$\boldsymbol{\Pi}_{\boldsymbol{\sigma}_2\boldsymbol{u}_2} = \begin{bmatrix} \left|\psi_0(\omega)\right|^2 \boldsymbol{I}_7 & \boldsymbol{0}_{7\times7} \\ \boldsymbol{0}_{7\times7} & -\boldsymbol{I}_7 \end{bmatrix}, \boldsymbol{\Pi}_{\boldsymbol{\sigma}_3\boldsymbol{u}_3} = \begin{bmatrix} \left|\psi_0(\omega)\right|^2 \boldsymbol{I}_7 & \boldsymbol{0}_{7\times7} \\ \boldsymbol{0}_{7\times7} & -\boldsymbol{I}_7 \end{bmatrix} \tag{41}$$

I_7 is identity matrix of order 7 and $\boldsymbol{0}_{7\times7}$ is zero matrix of order 7×7. Taking together the relations (36), (41), we get

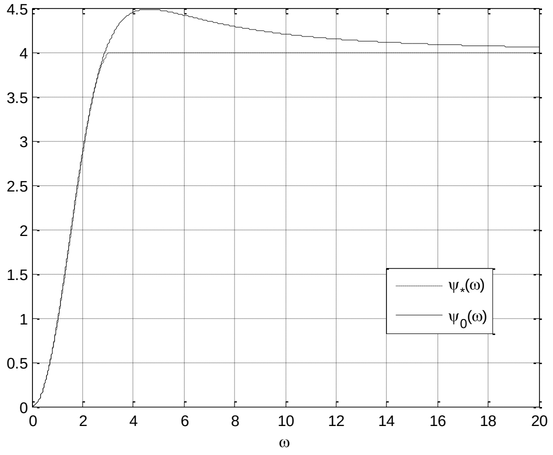

Fig. 8 – Finding an upper bound of mappings $\boldsymbol{\sigma}_2(t)\to \boldsymbol{u}_2(t), \boldsymbol{\sigma}_3(t)\to \boldsymbol{u}_3(t)$ gain

$$\begin{bmatrix} \hat{\sigma}_1(j\omega) \\ \hat{\boldsymbol{\sigma}}_2(j\omega) \\ \hat{\boldsymbol{\sigma}}_3(j\omega) \\ \hat{u}_1(j\omega) \\ \hat{\boldsymbol{u}}_2(j\omega) \\ \hat{\boldsymbol{u}}_3(j\omega) \end{bmatrix}^* \boldsymbol{\Pi}_{\boldsymbol{\sigma u}} \begin{bmatrix} \hat{\sigma}_1(j\omega) \\ \hat{\boldsymbol{\sigma}}_2(j\omega) \\ \hat{\boldsymbol{\sigma}}_3(j\omega) \\ \hat{u}_1(j\omega) \\ \hat{\boldsymbol{u}}_2(j\omega) \\ \hat{\boldsymbol{u}}_3(j\omega) \end{bmatrix} \geq 0$$

$$\boldsymbol{\Pi}_{\boldsymbol{\sigma u}} := \begin{bmatrix} 2 & 0 & 0 & 0 & 0 & 0 \\ \mathbf{0}_{7\times1} & |\psi_0(\omega)|^2 \boldsymbol{I}_7 & \mathbf{0}_{7\times7} & \mathbf{0}_{7\times1} & \mathbf{0}_{7\times7} & \mathbf{0}_{7\times7} \\ \mathbf{0}_{7\times1} & \mathbf{0}_{7\times7} & |\psi_0(\omega)|^2 \boldsymbol{I}_7 & \mathbf{0}_{7\times1} & \mathbf{0}_{7\times17\times7} & \mathbf{0}_{7\times7} \\ 0 & 0 & 0 & -1 & 0 & 0 \\ \mathbf{0}_{7\times1} & \mathbf{0}_{7\times7} & \mathbf{0}_{7\times7} & \mathbf{0}_{7\times1} & -\boldsymbol{I}_7 & \mathbf{0}_{7\times7} \\ \mathbf{0}_{7\times1} & \mathbf{0}_{7\times7} & \mathbf{0}_{7\times7} & \mathbf{0}_{7\times1} & \mathbf{0}_{7\times7} & -\boldsymbol{I}_7 \end{bmatrix} \in \boldsymbol{M}_{30\times30} \tag{42}$$

The matrix $\boldsymbol{\Pi}_{\boldsymbol{\sigma u}}$ defines an IQC of the problem of stability for the pilot-aircraft system with rate saturation and input delay (28).

Some preliminaries are necessary to establish the main result of the article. Let us note first that the matrix $\boldsymbol{\Pi}_{\boldsymbol{\sigma u}}$ can be written as the matrix product

$$\Pi_{\sigma u}(\omega) = H^*(j\omega) N H(j\omega) = \begin{bmatrix} H_1^*(j\omega) & 0 \\ 0 & I \end{bmatrix} \begin{bmatrix} I & 0 \\ 0 & -I \end{bmatrix} \begin{bmatrix} H_1(j\omega) & 0 \\ 0 & I \end{bmatrix} \tag{43}$$

$$H_1(j\omega) := \begin{bmatrix} \sqrt{2} & 0 & 0 \\ 0 & \psi_0(j\omega) I_7 & 0 \\ 0 & 0 & \psi_0(j\omega) I_7 \end{bmatrix} \tag{43'}$$

Considering (43), the condition (27) is successively rewritten as

$$\begin{bmatrix} G(j\omega) \\ I \end{bmatrix}^* \begin{bmatrix} H_1^*(j\omega) & 0 \\ 0 & I \end{bmatrix} \begin{bmatrix} I & 0 \\ 0 & -I \end{bmatrix} \begin{bmatrix} H_1(j\omega) & 0 \\ 0 & I \end{bmatrix} \begin{bmatrix} G(j\omega) \\ I \end{bmatrix} < 0$$

$$\begin{bmatrix} G^*(j\omega) & I \end{bmatrix} \begin{bmatrix} H_1^*(j\omega) & 0 \\ 0 & I \end{bmatrix} \begin{bmatrix} I & 0 \\ 0 & -I \end{bmatrix} \begin{bmatrix} H_1(j\omega) & 0 \\ 0 & I \end{bmatrix} \begin{bmatrix} G(j\omega) \\ I \end{bmatrix} < 0$$

$$\begin{bmatrix} G^*(j\omega)H_1^*(j\omega) & I \end{bmatrix} \begin{bmatrix} I & 0 \\ 0 & -I \end{bmatrix} \begin{bmatrix} H_1(j\omega)G(j\omega) \\ I \end{bmatrix} < 0$$

With the notations

$$L(j\omega) := G^*(j\omega)H_1^*(j\omega), W := \begin{bmatrix} I & 0 \\ 0 & -I \end{bmatrix} \tag{44}$$

we invoke further the Kalman-Yakubovich-Popov (KYP) Lemma in the version given in [49]:

Lemma 4.1. *The frequency domain inequality*

$$\begin{bmatrix} L(j\omega) \\ I \end{bmatrix}^* W \begin{bmatrix} L(j\omega) \\ I \end{bmatrix} < 0 \quad \forall\omega \in \mathbb{R} \tag{45}$$

holds if and only if there exists a matrix $P = P^{\mathrm{T}}$ *such that*

$$\begin{bmatrix} \tilde{A}^{\mathrm{T}}P + P\tilde{A} & P\tilde{B} \\ B^{\mathrm{T}}P & \end{bmatrix} + \begin{bmatrix} \tilde{C} & \tilde{D} \end{bmatrix}^{\mathrm{T}} W \begin{bmatrix} \tilde{C} & \tilde{D} \end{bmatrix} < 0 \tag{46}$$

where the four matrices $\left(\tilde{A}, \tilde{B}, \tilde{C}, \tilde{D}\right)$ *represent a realization of the transfer matrix* $\begin{bmatrix} L(s)^* & I \end{bmatrix}^*$.

The results of the article can be summarized as follows.

Proposition 4.3. *Let the problem of stability for the aircraft-pilot system described in the basic feedback configuration of IQC paradigm (Fig. 1), with the linear part defined by stable matrix* $\boldsymbol{G}$ *(35) and the "trouble makings" (saturation and delays) embedded in the nonlinear bounded causal operator* $\boldsymbol{\Delta}$ *(33), (3a). The bounded self-adjoint operator* $\boldsymbol{\Pi}_{\boldsymbol{\sigma u}}$ *(42) was chosen as IQC type multiplier. Let* $\boldsymbol{\Pi}_{\boldsymbol{\sigma u}}$ *have the realization*

$$\Pi = \begin{bmatrix} (j\omega I - A_\pi)^{-1} B_\pi \\ I \end{bmatrix}^* M_\pi \begin{bmatrix} (j\omega I - A_\pi)^{-1} B_\pi \\ I \end{bmatrix} \tag{47}$$

where $B_\pi = \begin{bmatrix} B_{\pi,x} & B_{\pi,w} \end{bmatrix}$ *and* A_π *is Hurwitz. Then the conditions 1) and 2) in Theorem 3.1 are fulfilled. The condition 3) is equivalent to the condition that the Riccati equation*

$$Q + PA + A^T P = (PB + S)R^{-1}\left(B^T P + S^T\right) \tag{48}$$

should have a stabilizing solution. The matrices in (48) are defined as

$$A=\begin{bmatrix} A_\pi & B_{\pi,v}C_G \\ 0 & A_G \end{bmatrix}_{30\times 30}, \quad B=\begin{bmatrix} B_{\pi,x}D_G + B_{\pi,w} \\ B_G \end{bmatrix}$$

$$\begin{bmatrix} Q & S \\ S^T & R \end{bmatrix} = -\left[\begin{array}{cc|c} I & 0 & 0 \\ 0 & C_G & D_G \\ \hline 0 & 0 & I \end{array}\right]^T M_\pi \left[\begin{array}{cc|c} I & 0 & 0 \\ 0 & C_G & D_G \\ \hline 0 & 0 & I \end{array}\right] \qquad (48')$$

A future work will consider numerical applications in order to prove the efficiency of the above theoretical developments.

REFERENCES

[1] A. I. Lurie, V. N. Postnikov, On the theory of stability of control systems, *Applied mathematics and mechanics*, **8**, 3, 1944, (in Russian).
[2] M. A. Aizerman, On a problem concerning stability „in the large" of dynamical systems (in Russian), *Uspekhi matematicheskikh nauk*, **4**, 4, pp. 187-188, August 1949.
[3] R. E. Kalman, Physical and mathematical mechanisms of instability in nonlinear automatic control systems, *Trans. ASME*, **79**, 3, pp. 553-563, Aprilie 1957.
[4] V. M. Popov, Absolute stability of nonlinear systems of automatic control, *Avtomatika i telemehanika,* **22**, 8, pp. 961-979, August, 1961.
[5] H. K. Khalil, *Nonlinear systems*, 3rd edition, Prentice Hall, 2002.
[6] V. Rasvan, D. Popescu, D. Danciu, Monotone and slope restricted nonlinearities – a PIO II case study, *Annals of the University of Craiova, Series: Automation, Computers, Electronics and Mechatronics*, **7 (34)**, 2, pp. 39-44, 2010.
[7] D. Materassi, M. Salapaka, M. Basso, A less conservative circle criterion, *Nonlinear Sciences – Chaos Dynamics*, June 2008; see also in *Proceedings of the 2006 ACC*, Minneapolis, Minnesota, USA, June 14-16, 2006.
[8] A. Megretski and A. Rantzer, System analysis via integral quadratic constraints, *IEEE Transactions on Automatic Control*, **42**, 2, pp. 819-830.
[9] U. Jönsson, *Lecture notes on integral quadratic constraints*, Department of Mathematics, KTH, Stockholm, 2000, ISBN 1401-2294. Available at http://www.montefiore.ulg.ac.be/services/systems/grad04/lecturenotes.pdf
[10] G. Zames and P. L. Falb, Stability conditions for systems with monotone and slope-restricted nonlinearities, *SIAM J. Control*, **6**, 1, pp. 89–106, March 1968.
[11] J. C. Willems, The least squares stationary, optimal control and thje algebraic Riccati equation, *IEEE Transactions on Automatic Control*, 16, 6, pp. 621-634, 1971.
[12] V. A. Yakubovich, Frequency domain for the absolute stability of systems containing several nonlinear or linear time invariant blocks (in Russian), *Avtomatika i Telemekhanika*, **31**, pp. 5–30, 1967.
[13] J. C. Doyle, Analysis of feedback systems with structured uncertainties, *IEE Proc.*, **D-129**, pp. 242-251, 1982.
[14] M. G. Safonov, Stability and robustness of multivariable feedback systems, *MIT Press*, Cambridge, MA, 1980.
[15] Vl. Rasvan, *Absolute stability of time lag control systems* (in Romanian), Romanian Academy Publishing House, 1975.
[16] F. Amato, R. Iervolino, S. Scala, L. Verde, Actuator design for aircraft robustness versus category II PIO, in *Proc. of the 7th Mediterranean Conference on Control and Automation [MED 99]*, Haifa, Israel, June 28-30, 1999.
[17] D. M. Klyde, D. G. Mitchell, A PIO Case study – Lessons learned through analysis. *AIAA Atmosphere Flight Mechanics Conference and Exhibit*, August 15-18, San Francisco, California, AIAA 2005-5813, 2005.
[18] E. P. Popov, *The dynamics of automatic control systems*, Pergamon Press, New York, 1962.
[19] H. J. Sussmann, E. D. Sontag, Y. D. Yang, A general result on the stabilization of linear systems using bounded controls, *IEEE Trans. on Automatic Control*, **39**, 12, pp. 2411-2425, 1994.
[20] R. A. Hess, Theory for aircraft handling qualities based upon a structural pilot model, *Journal of Guidance, Control, and Dynamics*, **12**, 6, pp. 792-797, 1989.
[21] D. L. Kleinman, S. Baron, W. H. Levison, An optimal control model of human response, Part 1: Theory and validation, *Automatica*, **6**, 3, pp. 357-369, 1970.

[22] S. Baron, D. L. Kleinman, W. H. Levison, An optimal control model of human Response, Part II: Prediction of human performance in a complex task, *Automatica*, **6**, 3, pp. 371-383, 1970.

[23] A. Toader, I. Ursu, Pilot modeling based on time delay synthesis, *Proceedings of the Institution of Mechanical Engineers - Part G: Journal of Aerospace Engineering,* **227**, 2013, doi:10.1177/0954410013478363.

[24] D. L. Kleinman, S. Baron, Manned vehicle systems analysis by means of modern control theory, *NASA CR-1753*, June 1971.

[25] J. B. Davidson, D. K. Schmidt, Modified optimal control pilot model for computer-aided design and analysis, *NASA Technical Memorandum 4384*, 1992.

[26] A. Toader, I. Ursu, From limits of human pilot mathematical modeling to actuator rate limits. A PIO II tendencies case study, *Mathematical Methods in Engineering, International Symposium-MME10*, Instituto Politecnico de Coimbra, Portugal, 21-24 October, 2010, CD published.

[27] A. Toader, I. Ursu, Towards a PIO II criterion: Improving the pilot modeling, in *Advances in Intelligent Systems and Computing*, vol. 187, 2013, pp 45-57, Springer-Verlag Berlin Heidelberg, 2013.

[28]] Z. Lin, Semi-global stabilization of linear systems with position and rate-limited actuators, *Systems & Control Letters*, **30**, pp. 1-11, 1997.

[29] H. Kwakernaak, R. Sivan, *Linear optimal control systems*, Wiley-Interscience, New York, 1972.

[30] W. M Wonham, On separation theorem of stochastic control, *SIAM Journal on Control and Optimization*, **6**, 2, pp. 312-336, 1968.

[31] M. Basin, *New trends in optimal filtering and control for polynomials and time-delay systems*, Springer-Verlag, Berlin Heidelberg, 2008.

[32] A. H. Jazwinski, *Stochastic processes and filtering theory*, Academic Press, New York, 1970.

[33] K. Ito, M. Nisio, On stationary solutions of a stochastic differential equations, *J. Math*., Kyoto Univ., 4, 1964, pp. 1–75.

[34] J. Lei, M. C. Mackey, Stochastic differential delay equation, moment stability, and application to hematopoietic stem cell regulation system, *SIAM Journal of Appl. Mathematics*, **67**, 2, pp. 387-407, 2007.

[35] B. Øksendal, *Stochastic differential equations. An introduction with applications*, Springer- Verlag, Berlin, New York, Tokio, Budapest, 1992.

[36] J. K. Hale, M. Sjoerd, V. Lunel, *Introduction to Functional Differential Equations*, Springer-Verlag, New York, 1993.

[37] T. Lauvdal, Stabilization of linear systems with input magnitude and rate saturations, *Thesis*, Depart. of Eng. Cybernetics, Norwegian Univ. of Science and Technology, Trondheim, Norway, 1998.

[38] I. Ursu, F. Ursu, F. Popescu, Backstepping design for controlling electrohydraulic servos, *Journal of The Franklin Institute*, **343**, January, 94-110, 2006.

[39] Tom Greetham, Evolution of Powered Aircraft Flight Controls, *MOOG Document*, pp. 1-31, February, 2012 (http://mae.osu.edu/sites/mae.web.engadmin.ohio-state.edu/files/uploads/ME888Presentations/evolution_of_powered_flight_controls_seminar.pdf)

[40] E. W. Vinje, D. P. Miller. Interpretation of pilot opinion by application of multiloop models to a VTOL flight simulator task, *NASA SP-144*, March, 1967.

[41] E. W. Vinje, D. P. Miller. An analysis of pilot adaptation in a simulated multiloop VTOL hovering task, *NASA SP-192*, March, 1968.

[42] A. Rantzer, A. Megretski, Analysis of rate limiters using Integral Quadratic Constraints, *Proceedings of IFAC Nonlinear Control Systems Design Symposium*, pp. 696-700, Enschede, Netherlands, 1998.

[43] L. G. Hofmann, K. V. Shah, D. Graham, Analysis of limited authority manual control systems, *TR AFFDL-TR-71-6*, July 1971.

[44] D. Materassi, M. V. Salapaka, Less conservative absolute stability criteria using Integral Quadratic Constraints, *American Control Conf.*, Hyatt Regency Riverfront, St. Louis, MO, USA, June 10-12, 2009.

[45] A. Megretski, Integral Quadratic Constraints for systems with rate limiters, *Technical Report LIDS-P-2407*, Massachussets Institute of Technology, Cambridge MA, December 1997.

[46] A. Chakraborty, P. Seiler, G. J. Balas, Local performance analysis of uncertain polynomial systems with applications to actuator saturation, *50th IEEE Conference on Decision and Control and European Control Conference (CDC-ECC)*, pp. 8176-8181, Orlando, FL, USA, December 12-15, 2011.

[47] G. Zames, P. L. Falb, Stability conditions for systems with monotone and slope-restricted nonlinearities, *SIAM Journal of Control*, **6**, 1, pp. 89-108, 1968.

[48] C.-Y. Kao, A. Rantzer, Stability analysis of systems with uncertain time-varying delays, *Automatica*, **43**, 959-970, 2007.

[49] M. C. Turner, M. Kerr, I. Postlethwaite, On the existence of stable, causal multipliers for systems with slope-restricted nonlinearities, *IEEE Transactions on Automatic Control*, **54**, 11, pp. 2697-2702, 2009.